Nano World Journal

https://doi.org/10.17756/nwj.2017-S1-003

Research Article

Open Access

Stability and Radiation Damage of Protein Crystals as Studied by Means of Molecular Dynamics and Monte Carlo Simulation

Philipp S. Orekhov[1*], Marine E. Bozdaganyan[2], Eugenia Peshkova[1,2] and Claudio Nicolini[2,3]

[1]Laboratories of Biophysics and Nanotechnology (LBN), University of Genova Medical School, Via Pastore 3, 16132 Genova, Italy
[2]Fondazione ELBA-Nicolini, Largo Redaelli 7, Pradalunga, 24020 Bergamo, Italy
[3]Nanoworld High Tech LLC, Boston, MA, USA

[*]Correspondence to:
Philipp S. Orekhov
Laboratories of Biophysics and Nanotechnology (LBN), University of Genova Medical School
Via Pastore 3, 16132 Genova, Italy
E-mail: ps.orekhov@gmail.com

Received: October 23, 2017
Accepted: December 18, 2017
Published: December 19, 2017

Citation: Orekhov PS, Bozdaganyan ME, Peshkova E, Nicolini C. 2017. Stability and Radiation Damage of Protein Crystals as Studied by Means of Molecular Dynamics and Monte Carlo Simulation. *NanoWorld J* 3(S1): S9-S14.

Published by United Scientific Group

Abstract

Molecular Dynamics (MD) and Monte Carlo (MC) simulations of crystals can help in interpretation of experimental X-ray crystallography data. Particularly, they can be useful for understanding how various crystallization techniques affect protein conformational plasticity within the crystal lattice and the stability of biomolecular crystals. The latter has become especially important since the modern and extremely intense X-ray radiation sources (such as free electron lasers, FELs) appeared recently.

In the present study we were able to show by means of computer simulations that the lysozyme crystals obtained using the Langmuir-Blodgett technique have an advantage over the classical ones ("Hanging Drop") in terms of their thermal stability as well as their stability against the radiation damage. We also demonstrate an important role of crystal water dynamics for stability of protein crystals.

Keywords

Molecular Dynamics (MD), Crystallography, Ionization, Monte Carlo (MC) simulations

Introduction

Modern X-ray crystallography is a dominant method for structure determination of large biomacromolecules such as proteins, nucleic acids and their complexes [1-3]. It allows to reconstruct atomic structure of biomacromolecular specimina with the atomic weights up to millions Da and with the resolution down to 1 Å, especially after appearance of such modern and extremely intense X-ray radiation sources as Free Electron Lasers (FELs). However, crystal stability and damage due to interactions of matter with the X-ray radiation limits time of diffraction data deposition and, thus, the resolution of the obtained electron density maps [4], which serve as a starting point for determination of the atomic positions.

It was previously shown using both *in vitro* and *in silico* approaches that the crystals obtained using the Langmuir-Blodgett (LB) technique have higher thermostability as well as higher stability against radiation damage in comparison with the classical Hanging Drop (HD) crystals and similarly to the Space-Grown (SG) crystals [3, 5]. However, it remains still unclear how and to which extend the shape and micrometer- and nanometer- scale structure of crystals, the methods utilized for the crystal growing influence the crystal stability particularly against the radiation damage.

MD simulations of proteins and other biomolecules in aqueous environments are now routinely performed at an atomic level on the time scale up to several microseconds. MD simulations have proved useful for multiple applications, including elucidating the origins of drug specificity, computing binding energies for ligand-protein systems [6], simulations of dynamics of proteins and biological membranes [7], etc. They also help to resolve such limitations of crystallographic studies as overreliance on static representation of biomolecular structure and inability to determine highly mobile molecules such as solvent. At the same time, the MC approach has gained wide acceptance in multiple fields of natural science and technology as an effective tool for rapid integration in the highly dimensional spaces. It is extensively utilized in nuclear physics, molecular modeling, elementary particle physics, analysis of the diffraction data, etc. [2, 8-10]. Particularly, the algorithms based on the MC approach are commonly used in femtosecond protein nanocrystallography. They allow to integrate Bragg intensities over the all possible nanocrystal orientations and sizes obtaining thus an electron density map from hundreds or even thousands of individual weak diffraction patterns [11].

In the present study, we combine the MC and MD simulations in order to track passage of highly energetic X-ray photons through protein crystals and assess the crystal stability. Particularly, this work aims to improve understanding of the exact organization of crystals and solvent orientation around the crystalized proteins. The important role of the latter was already discussed before [12]. Here, we address the problem of crystal stability directly using the MD simulations. For this purpose, we have carried out the MD simulations of the whole lysozyme crystals (extending the simulations carried out for individual lysozyme molecules before [5]) at different temperatures. Lysozyme is a ubiquitous protein, which appears in a plethora of organisms. It fights against the bacterial infection as it catalyzes bacterial cell wall lysis *via* hydrolysis of the β-1,4 glycosidic linkages between N-acetylmuramic acid and N-acetylglucosamine of peptidoglycan of the bacterial cell wall [13]. At the same time due to its small molecular weight and broad availability lysozyme serves as a model object for protein crystallography.

In this research we compared dynamics of lysozyme crystals obtained using the classical HD method, the LB method and the SG crystals. The optimized MD models of lysozyme crystals were subsequently used in simulations of the initial processes of radiational damage by means of the MC method as well as for estimation of crystal stability against radiation damage by means of the subsequent MD simulations.

Materials and Methods

For MD simulations we have chosen three structures of lysozyme representing different crystallization techniques: classical "hanging drop" (HD) – 3IJV, Langmuir-Blodgett (LB) – 2AUB and space-grown in the microgravity conditions (SG) – 1IEE. All crystallographic data is represented in table 1. The crystal triclinic supercell was set up for all models. Each cell contained 16 proteins, the total charge of such system was +128. The cells were solvated with the TIP3P water model and the chlorine ions were added in order to neutralize the systems. The parameters of the prepared in this way systems are shown in table 2.

Table 1: Experimental data about the selected crystal structures.

PDB ID	Symmetry	Cell size, nm×nm×nm	Cell angles	Resolution, nm
3IJV (HD)	43 21 2	7,6471×7,6471×3,6123	90×90×90	0,17
2AUB (LB)	43 21 2	7,9210×7,9210×3,7420	90×90×90	0,17
1IEE (SG)	43 21 2	7,7061×7,7061×3,7223	90×90×90	0,094

All simulations have been conducted in the GROMACS 2016 package using the CHARMM36 full-atom force field. All simulations were carried out at the desired temperature and 1 bar, which were maintained using the V-rescale (modified Berendsen) thermostat with a coupling constant of 0.1 ps and the Nose-Hoover barostat (isotropic, coupling constant of 2 ps). In the all of simulations the periodic boundary conditions were used. The time step was 2 fs. The Cutoff radius was setup to 1.0 nm for the Van der Waals and the short-range electrostatic interactions while for the long-range electrostatic interactions the PME method was used.

The equilibrium simulations were run for 100 ns at 300 K. After the equilibrium MD simulations, production MD simulations were carried out for 60 ns each at three temperatures – 300, 343 and 500 K. These temperatures were chosen as 300 K is the normal room temperature corresponding to the optimal conditions for lysozyme functioning, while two raised values of temperature were used to test the thermal stability of the protein crystals: 343 K is a bit lower than the thermal denaturation temperature for lysozyme (about 345-350 K depending on the solution content [14]) and 500 K is sufficiently above the thermal denaturation temperature.

The statistical significance of the differences was calculated by Student's t-test.

The optimized molecular models of protein crystals are

Table 2: Setup of the systems for MD simulations.

System	Initial volume of the simulation cell, nm^3	Total number of atoms	Number of water	Number of Cl- ions	MD simulation time, ns	
					Equilibrium MD: 300 K	Productive MD: 300 K, 343 K, 500 K
HD	481	50364	6292	128	100	60, 60, 60
LB	564	57108	8540	128	100	60, 60, 60
SG	541	54486	7666	128	100	60, 60, 60

imported into the MC simulation program code (Geant4 [15]) using a corresponding routine written by us in Python. The flowchart of the developed protocol for MC simulations is provided in figure 1. The effective cross-sections for interactions of photons with matter were set according to the NIST database.

On the next step, we provide the MC program (Geant4) with the full list of required simulation parameters, such as the list of accounted physical processes and parameters of the X-ray beam. In the present study, we consider the four processes, which happen during the radiation damage (see Figure 2): the photoelectric effect (which is a dominant process for the light elements such as the C, N, O, S atoms), with the consequent Auger electron emission, which results from the relaxation of electron from the high energy orbitals to the holes in the low energy orbitals appearing due to the photoeffect, the inelastic scattering (the Compton scattering, which is a dominant process for the H atoms) and the elastic scattering (which produces the diffraction pattern, however it is 20-30 times less probable than the photoeffect).

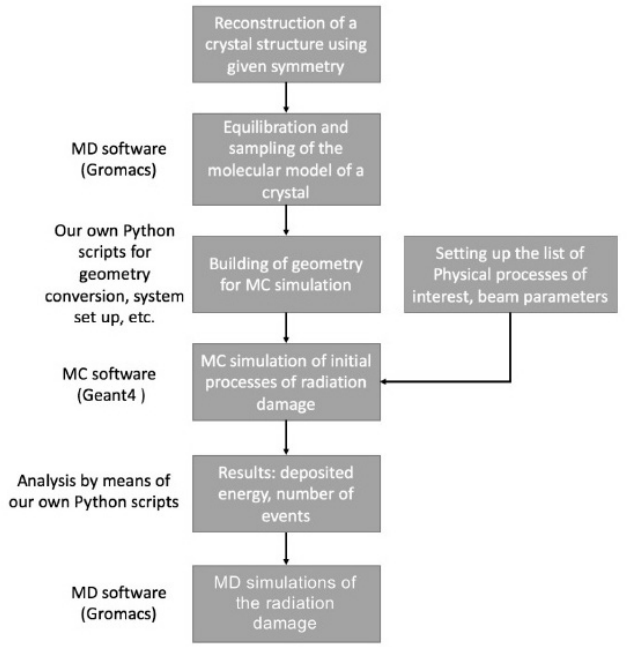

Figure 1: The workflow of a setup of a molecular system representing protein crystal and the subsequent MC simulation. In the left, the programs/tools used in the current procedure are shown.

The parameters of the beam were set in the way that photons were falling on the crystal from random positions but always from the same side of the crystal and perpendicular to it. All photons had identical and typical energy of a common X-ray synchrotron radiation beam, which equals 12.8 keV (~1 Å wavelength). The simulations were continued until the number of the elastic scattering events achieved the theoretical threshold required for a given resolution (13500 reflections for 2.0 Å).

Finally, the number of ionization events were drawn from the performed MC simulations. The analysis was done by the Python scripts.

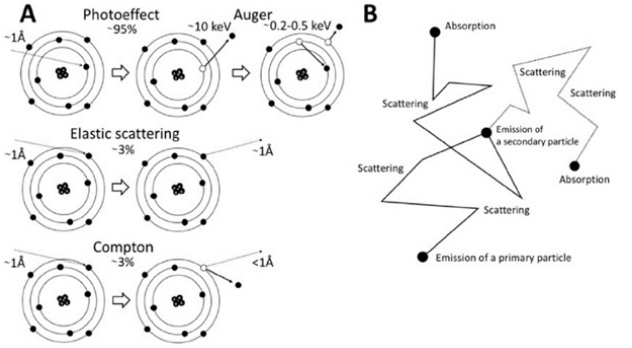

Figure 2: (A) Types of interaction of the X-ray photons with matter (electrons are shown as black cycles, electron holes as white cycles, photon tracks as dashed arrows, electron tracks as solid arrows). The four dominant processes are the Photoeffect, the Auger effect, the Elastic scattering (scattering without the loss of energy, which is responsible for diffraction) and the Compton scattering (scattering with the loss of energy). **(B)** Typical particle tracks as simulated by the Monte Carlo approach. Tracks (i.e., a particle path from the emission to the absorption) are shown for two particles, primary and secondary (which is produced due to interaction of a primary particle with matter).

The MD simulations of ionized proteins were carried out using the same computational protocol as for the simulations of thermostability. The ionization (according to the estimates done by MC simulations) was simulated as a random assignment of the +1 charges.

Results and Discussion

Thermostability of protein crystals

To investigate the effects of temperature on the protein conformational plasticity in the crystals obtained by different techniques (HD – the classical "hanging drop" technique, LB – the Langmuir-Blodgett technique, and SG – the space-grown crystals) and to elucidate possible determinants of their thermostability we have performed a series of MD simulations at different temperatures.

As can be seen, the structural parameters of all three crystals simulated at 300 K are similar and stable with the RMSD values fluctuating around 1.6-1.8 Å (Figure 3D-3F) and the gyration radius around 1.40-1.41 nm (Figure 3A-3C). However, already at this low temperature the volume and the crystal density differ significantly between all three systems (with p-values for all the pairs of observables below 10^{-250}, figure 5), what appears as an inherited property of the used crystal structures (Table 1): the HD crystal has the lowest volume and the highest density, while for the LB it is *vice versa*. Accordingly, we observed increased Lennard-Jones interaction energy between proteins in the HD crystal but not the electrostatic energy (Figure 6).

With the increase of the temperature the discrepancy in the stability of the three crystals emerge, both at the pre-denaturation temperature (343 K) and post-denaturation temperature (500 K) as appears evident from the plots of RMSD and gyration radius provided on figure 3 (p-values are

under 10^{-60} for all the pairs of observables). The LB crystal structure appears as the most stable in the all of the performed simulations.

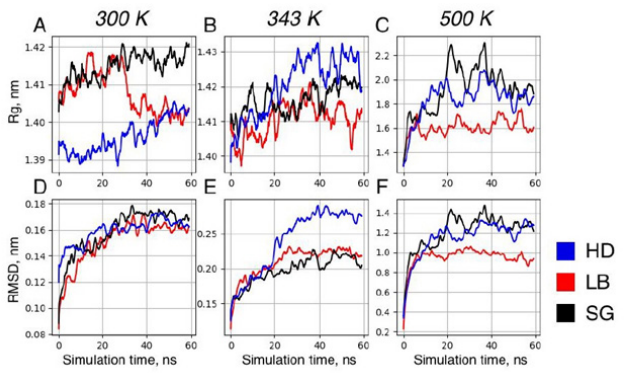

Figure 3: (A-C) Gyration radius averaged over 16 individual proteins in the crystal unit for the three systems (HD, LB and SG) simulated at three different temperature values (300, 343 and 500 K) plotted as a function of the simulation time; **(D-F)** RMSD averaged over 16 individual proteins in the crystal unit for the three systems (HD, LB and SG) simulated at three different temperature values (300, 343 and 500 K) plotted as a function of the simulation time.

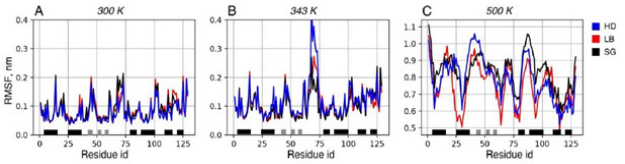

Figure 4: RMSF averaged over 16 individual proteins in the crystal unit for the three systems (HD, LB and SG) simulated at three different temperature values (300 K **(A)**, 343 K **(B)** and 500 K **(C)**) plotted as a function of residue index. The color bar in the bottom part of each plot indicates secondary structure elements, where α-helices are represented by black rectangles, β-sheets – by gray rectangles, while the rest corresponds to the fragments, which lack the secondary structure.

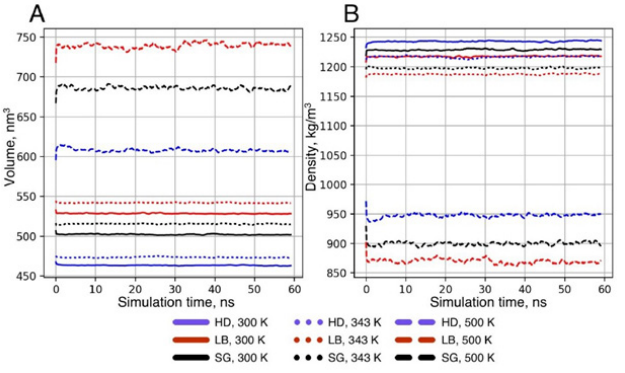

Figure 5: (A) Volume of the crystal unit for the three systems (HD, LB and SG) simulated at three different temperature values; **(B)** Density of the model crystal for the three systems (HD, LB and SG) simulated at three different temperature values.

At the level of individual amino acid residues, the difference in stability is seen both in the secondary structure elements and in the unstructured regions (see Figure 4) with the most contrasting variance in the loop region spanning residues 70-75, helical regions comprising residues from 25 to 30 and from 90 to 100. Thus, the difference in the stability can be attributed to the overall increased solidity of the protein structure, not just that of the secondary structure elements.

Since the major difference between the investigated crystal models is their volume and, as a consequence, the water content of them, we have investigated the water mobility in terms of the diffusion coefficient, D_{diff}, in all three systems at three different temperature values. The calculated diffusion coefficients of water molecules from the crystal simulations were compared with the water self-diffusion coefficients at the three studied temperatures (300, 343 and 500 K) obtained from a series of short MD simulations of a small water box (10 ns, 216 water molecules) at these temperatures.

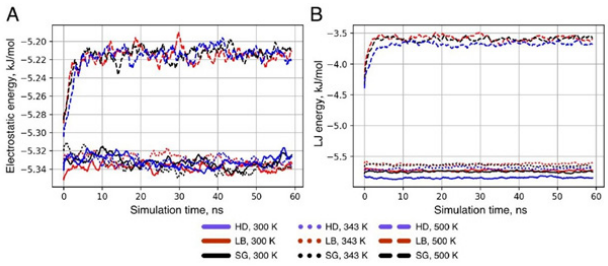

Figure 6: Protein-protein electrostatic **(A)** and Lennard-Jones **(B)** interaction energy plotted as a function of the simulation time for the three systems (HD, LB and SG) simulated at three different temperature values.

We have found out that in the LB and SG systems, which have the increased water content in comparison with the HD system, the distribution of the diffusion coefficients of water molecules has a noticeable shoulder at the higher D_{diff} values. This shoulder appears more prominent in the LB system than in the SG system, and its amplitude also increases with the temperature.

An apparent explanation of this observation is that the main peak of the D_{diff} distribution corresponds to the "slow" water molecules bound to proteins, while in the crystals with the bulkier unit cells (i.e., LB and SG) there appears an additional fraction of more mobile water molecules with the D_{diff} similar to the bulk water (compare solid curves to the dashed one on figure 7). These additional water molecular likely serve as a thermal bath, which draws heat from the protein molecules and, at the same time, separate them more

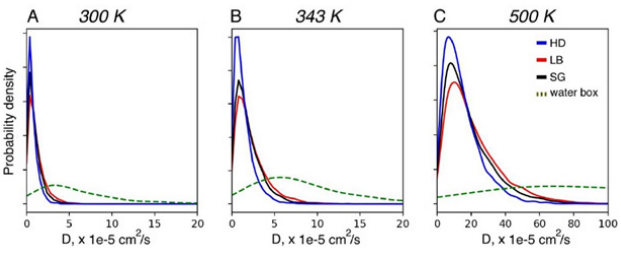

Figure 7: Distributions of the water diffusion coefficient calculated for the three systems (HD, LB and SG) simulated at three different temperature values (300 K **(A)**, 343 K **(B)** and 500 K **(C)**) along with the distributions of the water diffusion coefficient calculated from the short simulation of the pure water box (10 ns) at the corresponding temperature values.

efficiently, protecting them from the direct heat exchange and from the occurrence of the non-specific interactions (primarily Lennard-Jones as can be seen from figure 6B), which can lead to the structure loss and unfolding.

Radiation stability of protein crystals

The number of ionization events in protein crystals was estimated for crystal models of different sizes (the side of cubic crystal equaled 2.5 – 10 μm) using the final structures from the equilibration simulations of the LB and HD systems as a starting point. The ionization events were tracked using the MC approach as described in the Methods section.

We have found that the ratio of ionization events exponentially lowers with the increase of the crystal size in the investigated range of sizes (see Figure 8). In principle, two opposite effects of the crystal size on the radiation have to be considered: (1) smaller crystals need to be exposed to X-ray for a longer time in order to achieve sufficient scattering intensity; (2) the emitted highly energetic electrons leave smaller crystals easier. The damage was estimated by the number of the detected ionization events since it is known that the two major processes contribute to the crystal destruction: production of the free radicals and electrostatic repulsion of the ionized protein molecules [16]. Here, we intentionally neglected other effects of the synchrotron radiation on protein crystals, such as cleavage of specific bonds, etc. [4, 17], for the sake of simplicity of the obtained computer model. The observed dependence means that the effect of insufficient scattering intensity of smaller crystal is prevalent.

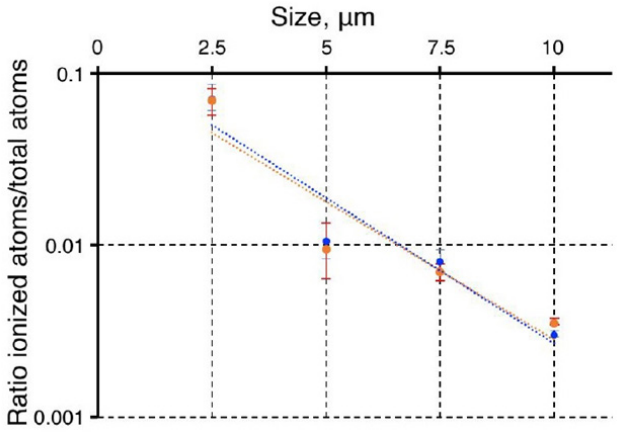

Figure 8: Ratio of ionized atoms (counted as a number of ionization events) to the total number of atoms in a system as a function of the system size.

Average values of the ionization rates obtained using the MC approach were further used to investigate the effects of ionization on the stability of the LB and HD crystals. We used two values for the fraction of the ionized atoms: 1/100 (corresponds to ~5 μm crystal) and 1/1000 (~10-100 μm crystal) of the total number of atoms. Ionization events were mimicked as a random assignment of the +1 charges to heavy atoms of the investigated systems. We employed a computational protocol and molecular systems similar to those described above for the estimation of thermostability. The length of all the performed simulations was 60 ns. The simulations were conducted at 300 K instead of the cryogenic temperature of 100 K typically used in real experiments [18] in order to accelerate the emergence of possible outcomes of ionization since elevated temperatures significantly improve sampling [19].

While no significant difference was observed in the simulations with the 1/1000 ionization fraction, when 1/100 of atoms were ionized we found a dissimilarity between the LB and HD systems in terms of RMSD and gyration radii (p-values are below 10^{-70} for both observables, figure 9) with the LB crystal model appeared more stable against ionization caused by the synchrotron radiation.

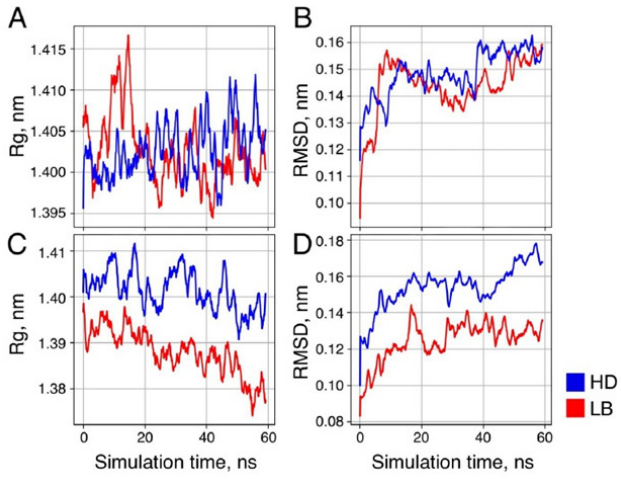

Figure 9: RMS deviations of atomic positions (RMSD) and gyration radii calculated for the LB (red) and HD (red) systems as a function of the simulation time: simulations with 1/1000 ionization rate **(A, B)** and 1/100 ionization rate **(C, D)**.

Conclusions

MD and MC simulations of the models of protein crystals obtained using various techniques (HD, LB and SG) have been used to investigate the effects of a crystallization technique on their conformational dynamics as well as thermal and radiation stability.

According to the results of our simulations at the room temperature there is no significant difference in stability of different crystals in terms of RMSD, the gyration radius or RMSF. However, they do differ in terms of the unit cell volume, density, the total water content and the interaction energy between the individual proteins within the crystal. With the increase of temperature to pre-denaturation and post-denaturation temperatures the space-grown and LB crystals are more stable than the classical HD one (for the LB crystals these results are confirmed by the previous experimental results obtained using circular dichroism, microGISAXS and bioinformatics analysis [3, 20]).

The observed thermostability of the LB and SG crystals is likely due to the higher content of the mobile water molecules, which can serve as a heat bath, which takes an excessive heat from proteins and, at the same time, split them apart more efficiently.

The increased thermal stability of the LB and SG crystals appears as a major contribution to the stability of crystals obtained by these techniques against the radiation damage as the later is largely attributed to the heating and burst of crystals upon their ionization.

Alongside, we have developed a computational protocol for efficient estimation of radiation damage in protein crystals by means of the MC simulations. The application of this procedure to the lysozyme crystals of various size showed that the number of ionization events exponentially lowers with the increase of the crystal size in the investigated range of sizes.

Combining the MC estimation of the ionization rate and the MD simulations for assessment of the crystal stability, we have shown that the LB crystals are also more tolerate to the electrostatical effects of ionization comparing to the classical HD crystals when the ratio of ionization events equaled 1/100 of the total number of heavy atoms, what can be especially important for the radiation stability of micrometer-scale crystals.

References

1. Nicolini C. 2009. Nanobiotechnology and Nanobiosciences: Pan Stanford Publishing, Singapore.
2. Nicolini C, Pechkova E. 2014. New trends in protein nanocrystallography based on LB nanotemplate, cell free expression, SNAP APA and montecarlo: a review. *Journal of Microbial & Biochemical Technology* 6(7): 366-369. https://doi.org/10.4172/1948-5948.1000170
3. Pechkova E, Bragazzi NL, Bozdaganyan M, Belmonte L, Nicolini C. 2014. A review of the strategies for obtaining high-quality crystals utilizing nanotechnologies and microgravity. *Crit Rev Eukaryot Gene Expr* 24(4): 325-339. https://doi.org/10.1615/CritRevEukaryotGeneExpr.2014008275
4. Weik M, Ravelli RB, Kryger G, McSweeney S, Raves ML, et al. 2000. Specific chemical and structural damage to proteins produced by synchrotron radiation. *Proc Natl Acad Sci U S A* 97(2): 623-628. https://doi.org/10.1073/pnas.97.2.623
5. Bozdaganyan M, Bragazzi NL, Pechkova E, Shaitan KV, Nicolini C. 2014. Identification of best protein crystallization methods by Molecular Dynamics (MD). *Crit Rev Eukaryot Gene Expr* 24(4): 311-324. https://doi.org/10.1615/CritRevEukaryotGeneExpr.2014010201
6. Bozdaganyan ME, Orekhov PS, Bragazzi NL, Panatto D, Amicizia D, et al. 2014. Docking and Molecular Dynamics (MD) simulations in potential drugs discovery: an application to Influenza virus M2 protein. *Am J Biochem Biotechnol* 10(3): 180-188. https://doi.org/10.3844/ajbbsp.2014.180.188
7. Bozdaganyan ME, Orekhov PS, Shaytan AK, Shaitan KV. 2014. Comparative computational study of interaction of C60-Fullerene and Tris-Malonyl-C60-Fullerene Isomers with lipid bilayer: relation to their antioxidant effect. *PLoS One* 9(7): e102487. https://doi.org/10.1371/journal.pone.0102487
8. Demarzo C, Distante A, Guerriero L, Niccolini C, Posa F, et al. 1975. A 4π scintillation counter-optical spark chamber system for neutral particles. *Nuclear Instruments and Methods* 131(1): 47-60. https://doi.org/10.1016/0029-554X(75)90355-9
9. DeMarzo C, Guerriero L, Nicolini C, Posa F, Vaccari E, et al. 1975. Differential cross sections for backward π− p→ nπ0 from 2.6 to 8 GeV/c. *Physics Letters B* 56(5): 487-490. https://doi.org/10.1016/0370-2693(75)90418-9
10. Lamanna E, Fiorillo A, Gallo A, Narciso A, Belmonte L. 2010. Dosimetric study in the human head for CT investigation of the inner ear using the Geant4 toolkit. *Nuclear Science Symposium Conference Record (NSS/MIC), 2010 IEEEI*. https://doi.org/10.1109/NSSMIC.2010.5874093
11. White TA, Kirian RA, Martin AV, Aquila A, Nass K, et al. 2012. CrystFEL: a software suite for snapshot serial crystallography. *Journal of Applied Crystallography* 45(2): 335-341. https://doi.org/10.1107/S0021889812002312
12. Pechkova E, Sivozhelezov V, Belmonte L, Nicolini C. 2012. Unique water distribution of Langmuir–Blodgett versus classical crystals. *J Struct Biol* 180(1): 57-64. https://doi.org/10.1016/j.jsb.2012.05.021
13. Kutter E. 2001. Lysozyme. In: Brenner S, Miller JF (eds) Brenner's Online Encyclopedia of Genetics. Academic Press, MA, USA, pp 1131-1132. https://doi.org/10.1006/rwgn.2001.0782
14. Sophianopoulos AJ, Weiss B. 1964. Thermodynamics of conformational changes of proteins. I. Ph-dependent denaturation of muramidase. *Biochemistry* 3(12): 1920-1928.
15. Agostinelli S, Allison J, Amako Ka, Apostolakis J, Araujo H, et al. 2003. GEANT4—a simulation toolkit. *Nuclear instruments and methods in physics research section A: Accelerators, Spectrometers, Detectors and Associated Equipment* 506(3): 250-303. https://doi.org/10.1016/S0168-9002(03)01368-8
16. Neutze R, Wouts R, van der Spoel D, Weckert E, Hajdu J. 2000. Potential for biomolecular imaging with femtosecond X-ray pulses. *Nature* 406(6797): 752. https://doi.org/10.1038/35021099
17. Duke E, Johnson L, Editors. 2010. Macromolecular crystallography at synchrotron radiation sources: current status and future developments. *Proceedings of the Royal Society of London A: Mathematical, Physical and Engineering Sciences*. https://doi.org/10.1098/rspa.2010.0448
18. Massover WH. 2007. Radiation damage to protein specimens from electron beam imaging and diffraction: a mini-review of anti-damage approaches, with special reference to synchrotron X-ray crystallography. *J Synchrotron Radiat* 14(1): 116-127. https://doi.org/10.1107/S0909049506052307
19. Day R, Bennion BJ, Ham S, Daggett V. 2002. Increasing temperature accelerates protein unfolding without changing the pathway of unfolding. *J Mol Biol* 322(1): 189-203. https://doi.org/10.1016/S0022-2836(02)00672-1
20. Pechkova E, Tripathi S, Nicolini C. 2009. MicroGISAXS of Langmuir–Blodgett protein films: effect of temperature on long-range order. *J Synchrotron Radiat* 16(3): 330-335. https://doi.org/10.1107/S0909049509002763